Title

Multiphase Distribution Feeder Reduction

Journal

IEEE Transactions on Power Systems, 33(2)

ISSN

0885-8950

Authors

Pecenak, Zachary K
Disfani, Vahid R
Reno, Matthew J
et al.

Publication Date

2018-03-01

DOI

10.1109/tpwrs.2017.2726502

Peer reviewed

Multiphase Distribution Feeder Reduction

Zachary K. Pecenak, Vahid R. Disfani, Matthew J. Reno and Jan Kleissl

***Abstract*—Quasi static time-series simulations (QSTS) of distribution feeders are a critical element of distributed solar PV integration studies. QSTS are typically carried out through computer simulation tools such as OpenDSS. Since a typical feeder contains thousands of buses, for long investigation periods or at fine time scales such simulations are computationally costly. Simulation times are reduced in this paper through a reduction of the number of buses in the model. The feeder reduction algorithm considers *p*-phase distribution feeders with unbalanced loads and generation, unbalanced wire impedance, and mutual coupling, while preserving the spatial variation of load and generation. An extensive Monte Carlo sensitivity analysis was performed on a real feeder from a California utility. All bus voltage differences are found to be less than 1.13% with a root mean square error of 0.21%. Simulation time savings were up to 96% when only one bus is selected to remain in the model. Example applications of the proposed algorithm are interconnection studies of utility-scale photo-voltaic system to the distribution grid, siting analyses of other distributed energy resources (DERs), and dynamic behavior of devices in large systems such as smart inverters on distribution grids.**

***Keywords*—Distribution system, network reduction, mutual impedance, quasi static time-series simulations, sky imager, spatio-temporal photovoltaic forecast.**

NOMENCLATURE

Λ_i	Ancestor set of bus i
Ω_i	Offspring set of bus i
$\overline{\overline{E}}$	Mean error of simulation
$\overline{E}_j$	Mean error of node j
$\phi(B_i)$	Phases of bus i
B_i	Bus in circuit
C_i	Children set of bus i
i, k, l	Index of bus
I_i	Current Injection at bus i
j	Index of phase on bus
m	Number of nodes, representing phases of bus
M_i	Set of nodes adjacent to nodes of bus i
n	Number of buses in feeder
N_i	Set of nodes of bus i
P_i	Parent of bus i
t_{red}	Time required to reduce feeder
t_{sim}^{day}	Time to simulate feeder for one day
t_{sim}^{year}	Time to simulate feeder for one year
W	Weight allocation matrix
w	Weight allocation sub-matrix
Z	Power Line Impedance Matrix
CB	Critical Bus, kept after reduction
NCB	Non-Critical Bus, removed during reduction

Zachary K. Pecenak and Jan Kleissl are with Department of Mechanical and Aerospace Engineering at University of California San Diego, La Jolla, CA 92093 USA {emails: zpecenak@ucsd.edu, jkleissl@ucsd.edu}

Vahid R. Disfani is with Department of Electrical Engineering at University of Tennessee at Chattanooga, Chattaooga, TN 37402 and with Center for Energy Research at University of California San Deigo, La Jolla, CA 92093 USA. {email: vahid-disfani@utc.edu}

Matthew J. Reno is with Sandia National Laboratories, Albuquerque, NM 8718 5USA {email: mjreno@sandia.gov}

I. INTRODUCTION

The aging infrastructure of the US electric grid combined with increasingly severe weather caused by climate change is threatening the reliability of electric delivery. Furthermore, the cost to rebuild and improve the infrastructure is putting pressure on tight state budgets [1]. This and environmental concerns have caused investor owned utilities (IOUs) and policy makers to invest in the next generation of grid deployable devices to improve reliability, voltage and frequency regulation, and advanced metering capabilities. Therefore, emerging technologies of distributed energy resources (DER) such as distributed photovoltaic (PV) systems, other distributed generators (DG), energy storage systems (ESS), and electric vehicle (EV) charging infrastructure will soon enter distribution grids at high penetrations.

In addition to evaluation of economic benefits and costs associated with integration of DER, their technical impacts such as voltage and frequency must be studied in realistic scenarios. Numerical simulations are generally easy to set up and allow investigations of a large number of configurations. However, a typical utility distribution feeder model contains a node for every customer and therefore consists of thousands of buses. While a single power flow completes after a few seconds on a workstation, consideration of multiple distribution feeders, large parametric analyses, or investigation at fine time scales, simulation time can become prohibitive. While previously it may have been sufficient for a utility to consider a mininimum and maximum load case to optimize voltage regulators to ensure voltage compliance, the emergence of high penetration of PV introduces challenges to this paradigm: (i) weather and seasonal variations of solar generation are typically examined using 8760 hourly times in a year (ii) some PV impacts such as tap operations can only be accurately benchmarked through simulation at time steps commensurate with tap operation control delays and cloud passages (seconds) (iii) worst cases are increasingly hard to define (high load and low solar and high solar variability), motivating a probabilistic framework for allocating future PV installations [2] and for decision-making in general.

So far, these scenarios have primarily materialized in distribution system research [3–5]. However, in the near future, utilities and their consultants will likely adopt these practices. DG interconnection studies performed by utilities on proposed installations that do not pass the initial screening requirements can then result in delays on the project due to long simulation

times [6, 7]. Further, in-depth studies of the dynamic and transient behaviors of several devices in complex systems are not feasible without the aid of super computers.

This dilemma has driven research to develop analytical methods to reduce the computational time required for large systems simulations while maintaining the accuracy of the solutions. A classical method for reducing system size is through the use of Kron reduction techniques, where buses with either no current or voltage are removed from the circuit [8]. While Krons reduction is valid and useful, the amount of reduction that is achievable in most systems is limited. Several authors have proposed reductions of the bulk electric transmission system through the use of equivalent collector systems, power injection matrix reduction, and bus aggregation [9, 10]. However, these methods fail to address the special characteristics of distribution systems such as multiphase connections, unbalanced loads, and mutual impedance.

Several other approaches in the literature propose analytical methods to entirely remove the need for a power flow solver. In [11], a method using base case circuit information is developed to find the optimal two-bus equivalent system of a transmission system for voltage stability analyses. Despite the high speed and accuracy of the method, the resulting circuit offers little flexibility to carry out investigations on other aspects of the power grid beyond transmission voltage stability. Another two-bus equivalent circuit formulation is proposed in [12] which is composed of a slack bus, equivalent impedance, and a single aggregated PV and load bus. The two-bus system allows quick and accurate investigation of voltage extrema in the circuit due to high variability of PV power output. However, the major drawback of this method is the fact that it is only able to simulate a single bus at a time and does not offer the flexibilitiy for comprehensive studies considering the coordinated behavior of several devices.

In addition to speeding up QSTS simulations, circuit reduction has been a research interest for several other applications. Specifically, methods have been proposed to reduce the circuit models for real-time control or hardware-in-the-loop (HIL) testing environments [13] that cannot handle the complexity and number of buses in a full distribution system model. Detailed dynamic analysis of large distribution systems is also often impractical in electromagnetic transient programs without network reduction [14]. With more DER being installed, there has also been a focus to expand the circuit reduction methods developed for equivalencing large wind farms for transmission dynamic [15], voltage ride-through [16], and harmonic studies [17]. These types of co-simulations with both transmission and distribution often reduce the complexity of the distribution system model by aggregating distributed generation into an equivalent dynamic model [18]

A novel methodology to reduce a balanced distribution feeder to any desired set of buses is presented in [19]. The methodology splits and aggregates load consecutively into neighboring buses using an impedance weighting. The accuracy of the method is tested against a 1000-node realistic feeder, where the maximum absolute deviation of voltage magnitudes between the reduced and original feeder is less than 10^{-3} V. However, as stated by the authors, the method is only applicable to simplified distribution networks without any unbalanced load or PV, unbalanced wire impedances, mutual coupling, or shunt capacitance. Moreover, in the load and PV aggregation process, the algorithm proposed in [19] does not consider the original positions of loads and PV to simulate of spatial variability. For these reasons, application of the methodology to real feeders results in large errors.

This paper builds upon [19] and resolves most of its limitations. An analytical method is proposed to reduce complex multiphase distribution feeders to a subset of buses (the critical buses (CB)) of interest. That is, the algorithm is applicable to *p*-phase distribution feeders with unbalanced loads and PV, unbalanced wire impedance, and mutual coupling between phases. The work is further extended through preserving the spatial diversity of solar and load on the circuit in the reduction process. The accuracy of the reduction is investigated on a real California feeder in reference to the complete simulation. Also, the sensitivity of voltage errors to location of the CB, types of loads, solar irradiance, PV penetration level, and bus distance from substation is investigated. Finally, the computational cost savings are quantified.

Thus, the contributions of this paper to the literature on network reductions are as follows:

1) Development of the first methodology to reduce real and complex distribution feeders which are unbalanced in nature. Such feeders can include:
   a) multiphase connections through out the entire network
   b) mutual coupling between multiphase unbalanced lines
   c) unbalanced loads and generation
   d) spatial variation in load and generation
2) The mathematical derivation and algorithm to implement the methodology are provided.
3) A novel methodology for aggregating temporal and spatial variation of load and generation across the network.
4) Development of a topology detection algorithm, which serves as a platform for manipulating values between buses.
5) Quantification of reduction errors for multiple load types, load conditions, and topology.

The rest of the paper is organized as follows. Section II explains the mathematical formulation of the reduction method. Section III proposes the algorithms to reduce the feeder to the desired CB. The simulation results and validation of the accuracy of the reduction method are provided in Section IV, along with a discussion on the computational advantages of the reduction. Section V concludes the paper.

II. Analytical Approach

A. Assumptions

We assume a radial network in a *p*-phase configuration with n buses and m nodes where a node refers to the individual phases of connections on a bus, such that $m \leq p{*}n$. For the purpose of clarity, the derivation and analysis is performed for a 3 phase system with multiphase connections (*p*=3).

Consistent with [19–22], the power injections and absorption on load and PV buses are assumed to be fixed current for the purpose of mathematical derivation (eq. 2-10). This assumption causes errors for constant PQ and constant impedance loads as well as for the PV systems which are typically modeled as constant PQ. The fixed current assumption is supported by research on conservation voltage reduction (CVR) [23], which showed that every 1% reduction in voltage leads on average to a 0.8% reduction in real power (CVR=0.8), while fixed current loads would cause CVR=1%. In spite of the error, methods using this assumption have shown to provide higher accuracy than other leading methods [24–26]. Further, the results provided in [27] demonstrate that the load type selected has minor effects on the simulation results.

However, it should be noted that the load types used in the feeder are kept during the aggregation process, as opposed to being changed to constant current. This is carried out by aggregating loads into groups of like load types in the final reduced feeder. The impacts of using different load types on the voltage error between the original and reduced feeder are investigated in Section IV.

In our work it is assumed that neutral connections could be provided by local grounding at any bus. Thus, the line models in this work do not include the neutral wire. In our algorithm, all loads are transformed to the equivalent Y-connected loads to derive the individual loads connected between each phase and ground. These loads define the equivalent single-phase loads on the reduced feeder. Further, the secondary side of the substation transformers are grounded and it remains the same in the reduced feeder since there is no reduction on transformers. Further, perfect grounding is assumed at each bus, thus neglecting the return current in the system, which can lead to inaccuracies under highly imbalanced conditions in models with imperfect grounding.

Finally, line capacitance is not treated in this model and assumed to be zero, thus rendering the method inaccurate for models with non-zero values. Reduction of shunt capacitance is a focus of future work.

B. Reduction Method

A bus is composed of several nodes N_i, representing the phases of connection. In a real multiphase distribution feeder, the number of phases between adjacent buses is often different, especially away from the main branch. Furthermore, PV and load on a bus are not necessarily evenly distributed between phases. The reduced feeder is required to maintain the original distribution of PV, load, and impedance by phase, thus it is necessary to aggregate the feeder at the phase level. Our comprehensive feeder reduction algorithm addresses all these special characteristics of distribution feeders.

The method proposed in this paper, which is based on defining the line impedance by Z matrices, is a highly generalized reduction technique applicable to distribution feeders with multiphase connections through out the entire network, mutual coupling between multiphase unbalanced lines , unbalanced loads and generation , spatial variation in load and generation It employs a recursive bus reduction technique which gradually removes non-critical buses (NCB) until only the set of selected CB remain (see section III-B). At every step, one NCB is removed and its load and PV systems are allocated between the adjacent CB, while total PV and load is preserved.

Fig. 1 shows the feeder structure at one of the intermediate feeder reduction steps in order to conceptualize the different types of reduction, which are described in Section III in detail. The objective in this feeder reduction is to remove the NCB while maintaining the voltage on the CB

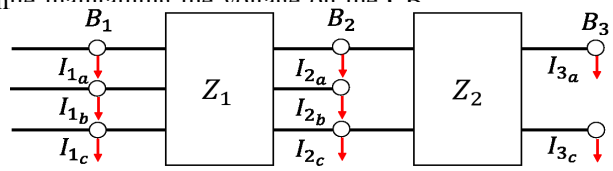

Fig. 1: Depiction of three bus subsection of the feeder in which the middle bus, B_2, is connected upstream to a 3 phase bus B_1 and connected downstream to a 2-phase bus B_3. The red arrows represent current flow out of the nodes.

Z_1 and Z_2 are multi-phase line impedance matrices, e.g.

$$Z_1 = \begin{bmatrix} Z_{1,aa} & Z_{1,ab} & Z_{1,ac} \\ Z_{1,ba} & Z_{1,bb} & Z_{1,bc} \\ Z_{1,ca} & Z_{1,cb} & Z_{1,cc} \end{bmatrix} \tag{1}$$

where the diagonal elements denote the self-impedances of all phases a, b, c and the off-diagonal elements are associated with the mutual impedance between different phases, which are not necessarily identical. The procedure is demonstrated through two scenarios;

C. Type 1: End bus Reduction

First, assume that buses B_2 in Fig. 1 is CB and the objective is to remove the bus B_3 which is NCB. If I_i and V_i respectively denote the 3-phase net current injection vectors and 3-phase voltage vectors on bus B_i, we have:

$$\begin{bmatrix} V_{3,a} \\ 0 \\ V_{3,c} \end{bmatrix} = \begin{bmatrix} V_{2,a} \\ 0 \\ V_{2,c} \end{bmatrix} - \begin{bmatrix} Z_{2,aa} & 0 & Z_{2,ac} \\ 0 & 0 & 0 \\ Z_{2,ca} & 0 & Z_{2,cc} \end{bmatrix} \times \begin{bmatrix} I_{3,a} \\ 0 \\ I_{3,c} \end{bmatrix} \tag{2}$$

$$\begin{bmatrix} V_{2,a} \\ V_{2,b} \\ V_{2,c} \end{bmatrix} = \begin{bmatrix} V_{1,a} \\ V_{1,b} \\ V_{1,c} \end{bmatrix} - \begin{bmatrix} Z_{1,aa} & Z_{1,ab} & Z_{1,ac} \\ Z_{1,ba} & Z_{1,bb} & Z_{1,bc} \\ Z_{1,ca} & Z_{1,cb} & Z_{1,cc} \end{bmatrix} \times \begin{bmatrix} I_{2,a} + I_{3,a} \\ I_{2,b} \\ I_{2,c} + I_{3,c} \end{bmatrix}. \tag{3}$$

From (2) and (3) the voltage vectors V_1 and V_2 can be written as functions I_2 and I_3 which exclude V_3. Therefore, the bus B_3 can be removed from the feeder by just transferring its current injections to B_2.

D. Type 2: Middle Bus Reduction

In this type of reduction, B_1, B_2, and B_3 are three consecutive buses in one of the intermediate reduction steps where B_2 is the NCB to be removed, B_3 is CB, and B_1 can be a CB or NCB. Without loss of generality, let us assume a special case where the line between B_2 and B_3 is also three-phase, *i.e.* $Z_2 \in \mathbb{C}^{3\times3}$. Thus, we have:

$$V_3 = V_2 - Z_2 \times I_3 \tag{4}$$

$$V_2 = V_1 - Z_1 \times (I_2 + I_3). \tag{5}$$

Replacing voltage parameters corresponding to B_2 by the parameters of the neighboring buses, the voltage vector V_3 is represented as below

$$V_3 = V_1 - Z_1 \times (I_2 + I_3) - Z_2 \times I_3 = V_1 - (Z_1 + Z_2) \times (I_3 + (Z_1 + Z_2)^{-1} \times Z_1 \times I_2), \quad (6)$$

which implies a single three-phase line between B_1 and B_3 with an impedance matrix equal to Z_{eq}=Z_1+Z_2, while the new load at B_3 includes a portion of load from the removed bus in addition to its original load. Due to the symmetry of the example network, the load on bus B_1 must be updated to I_1+$(Z_1$+$Z_2)^{-1} \times Z_2 \times I_2$. Therefore, total feeder loads remain the same.

In general, if any of the lines between the original buses lack some phases, the process is slightly different. In such conditions, the equivalent line includes only the common phases between Z_1 and Z_2. All loads on the phases which are just connected to one of adjacent buses must be transferred to the same phase of that bus.

As a general case, it is assumed here that the number of phases of the lines Z_1 and Z_2 are not the same, *e.g.* $Z_1 \in \mathbb{C}^{3\times3}$ and $Z_2 \in \mathbb{C}^{2\times2}$. These lines connect three buses with phase nodes $\phi(B_1) = \{a, b, c\}$, $\phi(B_2) = \{a, b, c\}$, and $\phi(B_3) = \{a, c\}$ as depicted in Fig. 1. For a NCB with multiphase connections, such as the given example, it is necessary to identify the phases common and not common to both lines.

To avoid zero determinants in the inversion of Z_{eq}, a reduced verion of the matrices is introduced. Assuming that Z_1^r and Z_2^r are the reduced format of Z_1 and Z_2 which only includes the elements corresponding to phases $\{a, c\}$=$\phi(B_1) \cap \phi(B_2) \cap \phi(B_3)$, the equivalent impedance is equal to $Z_1^r + Z_2^r$, as defined in (7).

$$Z_{eq} = \begin{bmatrix} Z_{1,aa} & Z_{1,ac} \\ Z_{1,ca} & Z_{1,cc} \end{bmatrix} + \begin{bmatrix} Z_{2,aa} & Z_{2,ac} \\ Z_{2,ca} & Z_{2,cc} \end{bmatrix} \quad (7)$$

Since there is no connection between B_1 and B_3 through the uncommon phase, any elements corresponding to this phase in the equivalent impedance disappear.

For uncommon phases, all load and PV connected to the middle bus are transferred to the bus which includes the uncommon phase. For example, all load and PV on phase b of bus B_2 are transferred to phase b of bus B_1 (Fig. 1). However, the load and PV on common phases of the middle bus are allocated between the other two buses according to the impedance matrices of Z_1^r and Z_2^r.

$$\begin{bmatrix} I_{3,a} \\ I_{3,c} \end{bmatrix}^{\text{new}} = \begin{bmatrix} I_{3,a} \\ I_{3,c} \end{bmatrix} + Z_{eq}^{-1} \times \begin{bmatrix} Z_{1,aa} & Z_{1,ac} \\ Z_{1,ca} & Z_{1,cc} \end{bmatrix} \times \begin{bmatrix} I_{2,a} \\ I_{2,c} \end{bmatrix} \quad (8)$$

$$\begin{bmatrix} I_{1,a} \\ I_{1,c} \end{bmatrix}^{\text{new}} = \begin{bmatrix} I_{1,a} \\ I_{1,c} \end{bmatrix} + Z_{eq}^{-1} \times \begin{bmatrix} Z_{2,aa} & Z_{2,ac} \\ Z_{2,ca} & Z_{2,cc} \end{bmatrix} \times \begin{bmatrix} I_{2,a} \\ I_{2,c} \end{bmatrix} \quad (9)$$

$$I_{1,b}^{\text{new}} = I_{1,b} + I_{2,b} \quad (10)$$

E. PV and load allocation

To aggregate time-series load shapes a complex matrix $W \in C^{(3n\times3n)}$ maps the PV or load from nodes of NCB to the CB nodes which it is transferred to. The elements W_{jj} are initialized as 1 if there is a PV/load on that node, and it is 0 otherwise. In each step of feeder reduction W is updated to represent the contribution of PV/load from the removed NCB onto the phases of the CB and rows corresponding to NCB are removed.

For middle bus reduction we define the ratio matrices $R_1 \in \mathbb{C}^{3\times3}$ and $R_2 \in \mathbb{C}^{3\times3}$. Matrix elements corresponding to the common phases between the three buses are equal to elements of the reduced matrices, $R_1^r = Z_{eq}^{-1} Z_2^r$ and $R_2^r = Z_{eq}^{-1} Z_1^r$. For the elements of R_1 and R_2 corresponding to the uncommon phases off-diagonal elements are all zero, except elements corresponding to common phases with only bus, in which the element is one. For the example shown in Fig. 1 the ratio matrices R_1 and R_2 are:

$$R_1 = \begin{bmatrix} r_{1,aa}^r & 0 & r_{1,ac}^r \\ 0 & 1 & 0 \\ r_{1,ca}^r & 0 & r_{1,cc}^r \end{bmatrix}, R_2 = \begin{bmatrix} r_{2,aa}^r & 0 & r_{2,ac}^r \\ 0 & 0 & 0 \\ r_{2,ca}^r & 0 & r_{2,cc}^r \end{bmatrix} \quad (11)$$

The ratio matrices R_1 and R_2 express how load and PV on the middle bus are allocated between the other buses:

$$w_{B_1} = w_{B_1} + R_1 \cdot w_{B_2}, w_{B_3} = w_{B_3} + R_2 \cdot w_{B_2} \quad (12)$$

The weight submatrices $w \in \mathbb{C}^{3\times3}$, corresponding to the elements of W representing the two CBs are updated to reflect the phase-wise addition of PV/load from the NCB (B_2) whose rows are removed.

For end bus reduction where B_3 is to be removed, w_{B_2} will be updated to $w_{B_2} + w_{B_3}$ and the rows corresponding to B_3 are removed.

Following the reduction to the final set of nodes, W can be used to map the original PV/load time series profiles to the reduced set.

III. Feeder Reduction Algorithm

A. Introduction

The steps of the feeder reduction of a large and complex distribution feeder are broken out next. The procedure of bus selection by the user and the algorithm is discussed (section III-B). The steps of recursively removing NCB from the branches of the feeder following the analytical approach of section II-C is given in section III-C. A novel approach to handling the reduction between multiphase connections with mutual coupling is discussed in section III-D based on the methodology of section II-D. The weighting system to maintain solar and load variability proposed in II-E is implemented in section III-E.

B. Critical Bus Selection and Identification

CB are defined as the buses that are to remain in the final reduced feeder configuration. While the number of CB can range from one bus to all of the buses, generally CB are a small

subset of the total buses of the feeder. There are three types of CB; i) user-selected CB, ii) CB that host special equipment, and iii) topology CB.

User-selected CB are those of interest to the particular study being performed, such as the location where a large PV system is to be interconnected. CB that host special equipment are buses with shunt capacitors, voltage regulators, and distribution transformers, which are automatically classified as CB.

Based on this initial set of CB, the algorithm must select additional CB which are required to preserve the topology of the feeder. Topology CB are buses on the junctions between branches with CB. The algorithm identifies the topology of the feeder to determine where the user-selected CB or CB with special equipment are located, selects the topology CB, and determines which buses must be removed. A modified version of the recursive topology detection algorithm proposed in [28] has been adopted in this paper.

In the method, adjacent buses to any bus i, as identified through connected phases in the line data or the admittance matrix, form the full set of neighbor buses N_i. Among the neighbors of bus i, the closest one towards the substation is called the parent of bus i (P_i). The remaining buses of N_i form its children set C_i. The offspring set of bus i, denoted by Ω_i, is recursively defined as the union of the children of bus i (C_i) and their offspring set i.e. $\Omega_i = C_i \bigcup (\bigcup_{k \in C_i} \Omega_k)$. The ancestor set of bus i, which is denoted by Λ_i, also has a recursive definition of the bus i's parent and its parent's ancestors, *i.e.* $\Lambda_i = P_i \bigcup \Lambda_{P_i}$.

The full algorithm is presented in **Algorithm 1**. The algorithm starts from the substation ($i = 1$), finds its children and updates the sets of global variables Λ and Ω. The algorithm is then repeated for each child until the entire network is processed.

Algorithm 1 Topology Detection

Initialize $\Lambda_i = \emptyset$ and $\Omega_i = \emptyset$
identify any bus connected to bus i to form the neighbor set M_i.
Define the children set $C_i = \{k : k \notin \{i\} \cup \Lambda_k\}$
for any bus l in C_i **do**
  let $P_l = i$ and $\Lambda_l = \{i\} \cup \Lambda_i$
  let $i = l$ and run **Algorithm 1**
  $\Omega_{P_i} = \Omega_{P_i} \cup \{i\} \cup \Omega_i$
end for
Return the sets Λ_i and Ω_i

After the feeder topology is detected, among the common ancestors of each pair of critical buses, the one with higher distance from the substation is considered as the junction of those two critical buses and is added to the list of critical buses. It is notable that the substation bus must be always a critical bus.

C. Branch Reduction, End Bus

Following the concept of graph theory the feeder is considered as a tree where the buses and distribution lines are equivalent to vertices and edges, and the part of the feeder that interconnects the CB is the main tree which just includes the ancestors of all critical buses. The first objective in the feeder reduction algorithm is to remove all NCB off the main tree. The loads and PV on these NCB are aggregated on the closest CB belonging to the main tree.

Algorithm 2 elaborates how the buses off the main tree are reduced, where $w_i \in \mathbb{R}^{(3\times n)}$ consists of three rows of the matrix of W corresponding to the different phases of bus i.

Algorithm 2 Reduction Off Main Tree

Identify the feeder topology (obtain the sets Λ_i and Ω_i for all buses i)
Form the set of CB
Form the set of all buses on the main tree, $T = \bigcup_{i \in CB} \Lambda_i$
Initialize the set of NCB: $R = \emptyset$
for any CB $i \in T$ **do**
  for any $l \in C_i$ if Ω_l excludes any critical bus **do**
    let $R = R \cup \{l\}$, $w_i = w_i + w_l$, and $w_l = 0$
    for any bus k downstream of bus i $(k \in \Omega_l)$ **do**
      let $R = R \cup \{k\}$, $w_i = w_i + w_k$, and $w_k = 0$
    end for
  end for
end for
Remove the buses belonging to R from the feeder
Remove the row vectors w_r from matrix W for any $r \in R$

Fig. 2 also illustrates a case where the buses off the main tree are reduced on the CB. After this step, the remaining feeder includes all CB and some NCB which reside on the main tree.

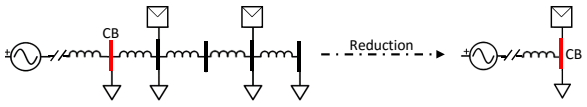

Fig. 2: A conceptual depiction of the removal of all NCB beyond a CB. The load (triangles) and PV (squares) from the removed NCB are aggregated to the CB. This process is carried out recursively for all CB off the main tree.

D. Main Tree Reduction, Middle Bus

The impedance that connects the remaining buses composes the characteristic impedance of the reduced circuit and thus must be aggregated as opposed to removed. The methodology as described in II-D is shown for a simple three bus system, but for larger feeders the process is carried out in the reduction by successively removing NCB parents of CB until the NCB are completely removed from the circuit. **Algorithm 3** summarizes the reduction of the NCB on the main tree.

E. The Final Reduced Feeder

The final configuration contains only CB which are connected through a set of equivalent distribution lines. Fig. 3 displays the CB identified by the algorithm following the user-selection of nine CB. The algorithm chose on additional CB due to the presence of a capacitor and 9 topological CB.

The CB are composed of nodes with various weighting vectors. The final matrix W is used both to calculate the equivalent

Algorithm 3 Reduction On Main Tree

Identify the new feeder topology reduced by **Algorithm 2**
Form the set of CB
Initialize the set of NCB: $R = \emptyset$
for any $i \in$ CB **do**
  Sort Λ_i based upon distance from substation ascendingly
  for any $k \in \Lambda_i$ (in order) **do**
    if $((\{k\} \bigcup \Omega_j) - (\{i\} \bigcup \Omega_i))$ which excludes any CB **then**
      let $w_i = w_i + R_2 \cdot w_k$ and $w_{P_k} = w_{P_k} + R_1 \cdot w_k$
      let $w_k = 0$ and $R = R \bigcup \{k\}$
    end if
  end for
end for
Remove the NCB belonging to R from the feeder
Remove the row vectors w_r from matrix W for any $r \in R$

PV and load sizes and to compute the aggregate generation and demand profiles on the final set of CB. Normalizing the generation and demand profiles based on the equivalent sizes of PV and load generates the temporal PV and load loadshapes. The reduced system contains less PV generators with larger individual capacities than the original system.

An executable to run the feeder reduction code has been uploaded to [29]. Details of the operations and limitations are given there.

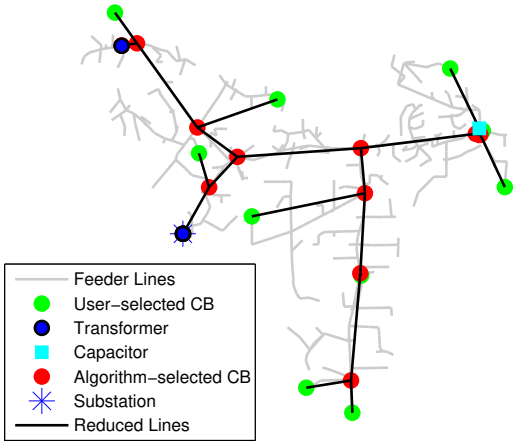

Fig. 3: Reduced (black) California distribution feeder overlayed on the full distribution feeder (grey). Initially nine buses were user-selected as CB and the algorithm selected the additional buses.

IV. Validation

A. Distribution Feeder

To evaluate the accuracy of the proposed circuit reduction algorithm, a stochastic sensitivity analysis was performed on a real medium voltage (MV) California distribution feeder with 621 multi-phase buses, two distribution transformers, one large capacitor bank (1350 KVAr), 364 distributed rooftop PV systems, and 471 loads. Each load operates under the same time-series shape scaled by its peak load, while each PV time-series is uniquely determined using a sky imager according to the method introduced in [4]. The feeder lines are modeled with zero shunt capacitance, and all neutral connections are assumed to be grounded perfectly. Feeder reduction simulations are run in OpenDSS [30] for one day with a time resolution of 30s.

A one-year QSTS with 1-minute resolution for each solar deployment is the standard simulation setting that DOE considers for solar planning studies to capture effects of PV fluctuations [7]. Therefore, one-year QSTS simulations with 30-sec resolution in this paper is commensurate with the minimum requirements set by DOE. Given that these standards will guide academia and industries in future solar planning for both research and implementation projects; the authors conclude that these settings are relevant to show the reduction of the computation expenses through the proposed algorithm.

B. Sensitivity Analysis

1) Error metrics: Given the importance of voltage in QSTS simulations, errors are defined as the difference in voltage of each CB from the identical node in the full feeder configuration: $E_j(t) = V_{\text{full}_j}(t) - V_{\text{reduced}_j}(t)$, where j indicates a node, and t indicates a time step. Mean $(\overline{E_j}, \overline{\overline{E}})$ absolute error metrics are used to elucidate the voltage difference as a function of the different circuit configurations:

$$\overline{E}_j = \frac{1}{T}\Sigma_{t=1}^{T}|E_j(t)| \tag{13}$$

$$\overline{\overline{E}} = \frac{1}{J}\Sigma_{j=1}^{J}|\overline{E}_j| = \frac{1}{J}\frac{1}{T}\Sigma_{j=1}^{J}\Sigma_{t=1}^{T}|E_j(t)| \tag{14}$$

2) Simulation scenarios: The sensitivity to the following feeder conditions was analyzed: (i) Two days with the highest (01/18/2015) and lowest (12/26/2014) aggregate load; (ii) PV generation profiles from a mostly clear day (12/19/2014) and a day with overcast clouds in the morning and partly cloudy conditions in the afternoon (12/12/2014); (iii) PV penetrations of 50% and 100% where PV penetration is defined as the ratio between the installed rated PV capacity and the peak rated load on the feeder and is increased/decreased by scaling each PV system up or down by the same factor; (iv) Three different load types (constant-power, constant-impedance, and fixed-current magnitude) to observe the effect of deviating from the fixed current load used in which the algorithm. It is worth mentioning that the fixed-current magnitude load type used in OpenDSS differs from the assumption of fixed complex current which is used in the derivation.

The combination of these conditions results in $(2\times2)\times2\times3$ = 24 feeder configurations.For each of these 24 baseline configurations, 1,000 reduction simulations are run. For each reduction simulation, the number of user-selected CB is randomly selected between 2 and 50. The CB locations are also randomly selected. Topology CB are then selected by the algorithm as described in section III. The three buses with distribution transformers or capacitor banks are always CB.

Over all j and all configurations (24,000 simulations and on average 28 CB per simulation) the root-mean square deviation (RMSD) is 2.11×10^{-4} p.u., mean bias error (MBE) is 3.46×10^{-4} p.u., and the maximum observed error is 0.0113 p.u. (or 1.13%).

3) Sensitivity load type: Fig. 4 gives the histogram of errors for all simulations of each load type. Each load exhibits a strong peak around 0 error and errors greater than $\pm 1 \times 10^{-3}$ p.u. occurs for less than 0.5% of all nodes. Overall the difference in error imposed by using different load types is small. Contrary to the expected behavior, the largest peak at zero error occurs for the constant power load types, followed by constant current load types and then constant impedance load types. The increase in error for constant current load types is due to the fact that the derivation assumes the current is constant in both magnitude and angle, where the OpenDSS models fixed current magnitude only.

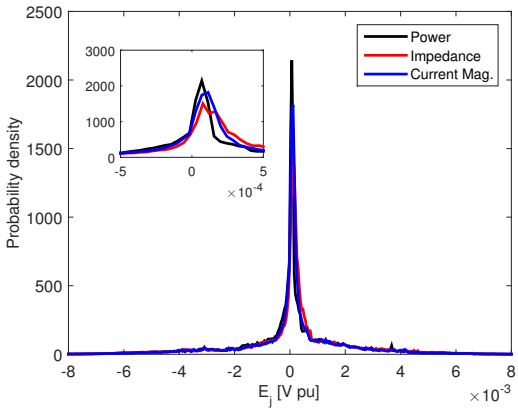

Fig. 4: PDF of error for each load type. All nodes in each simulations corresponding to each load are represented in the function (i.e 8,000 simulations $\times$ $\approx$50 nodes). The inset plot provides a zoomed view of the histogram with x-axis limits of $\pm 5 \times 10^{-4}$

4) Sensitivity to loading: When comparing error as a function of the node net load (Fig. 5) we again see little change in error as a function of load type used. For all load types, the lowest error is seen for buses with near zero net load. As the net load deviates from zero, the error increase with some symmetry in both directions. The increase for large positive and negative net load is indicative of the constant current assumption used being a significant source of error, which is more noticeable for large amounts of generation/consumption.

5) Sensitivity to distance: Finally, mean error as a function of distance from the substation (Fig. 6), supports the conclusion that the load type has little effect on the error. However, we do see a strong correlation with increasing distance away from the substation. This behavior is consistent with intuition since the voltage at the substation is a set value dependent on the upstream conditions, whereas buses at the end of the feeder are subject to an accumulation of reduction error.

6) Sensitivity to number of critical buses: 1,000 additional simulations were performed by randomly selecting number and location of CBs with the number ranging from 1 to the full set of 621. Given the small sensitivity to the parameters considered in the previous section, the analysis is carried out with constant impedance loads (highest error) on 12/26/2014. Figure 7 shows that, as expected, the error in voltage decreases as less buses are removed from the circuit. Non-zero error is noticed for the case of zero buses removed (i.e. the circuit is re-written

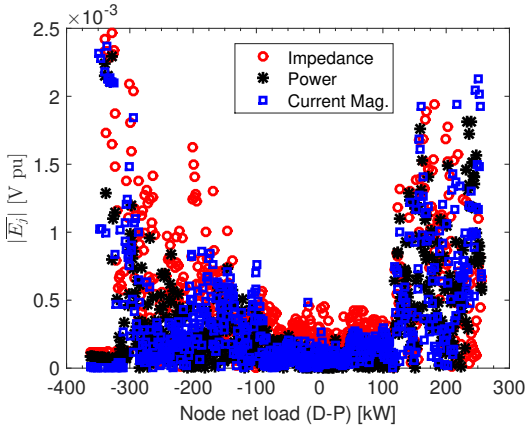

Fig. 5: Mean error of node voltage plotted as a function of net load on the bus. The mean is taken by binning all net loads in 1 W bins and averaging all errors in the bin.

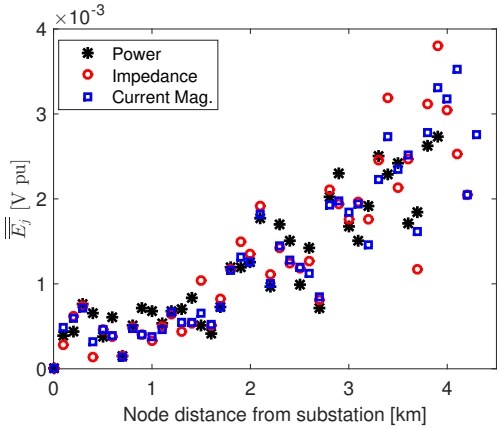

Fig. 6: Mean error of node voltage plotted as a function of distance of the node from the substation. The mean is taken by binning all nodes into 100m bins and taking the average of all nodes in that bin across all simulation time steps.

with no modification), as a result of the stopping criteria of the solver.

C. Computational Expense

Since the ultimate objective of feeder reduction is increased computational speed, the computational cost associated with reducing and simulating different sized feeders was investigated. Simulations were run on a desktop with an Intel(R) Core(TM) i7-4770 processor and 32 GB RAM. Fig. 8 plots the computational time required to reduce the 621 bus feeder as well as the computational time to simulate a full day of QSTS at 30 s resolution for the resulting feeder. Both lines show an increase in time with an increase in the number of buses remaining in the system with slopes 0.18 and 0.021 seconds/bus for reduction and simulation, respectively.

Fig. 8 indicates that the time to reduce the feeder is about 9 times that of a short QSTS simulation run. However, the reduction time is a one-time cost which quickly pays back when long-term or parametric studies are conducted. For year long simulations at 30 s resolution (Table I) simulation time decreases by 31% for only a 20% reduction of buses. Savings

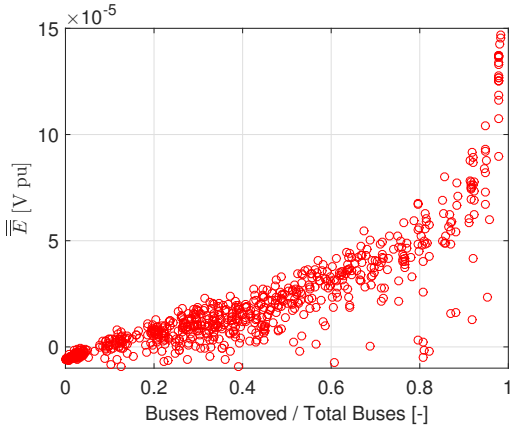

Fig. 7: Average daily error plotted against the total number of buses removed in the simulation. Each point corresponds to error averaged across all time steps and all buses in each simulation, as defined by equation 14. 1,000 simulations were configured under HS50 with constant impedance loads.

greater than 90% are observed for system that reduce 96% of buses. At 621 buses the present feeder was relatively small; larger relative computing time savings are expected for larger feeders. It is noted, t_red increases as fewer buses are reduced. The increase in time is a result of the structure of the algorithm which loops through each bus CB during each step of the reduction. More CB leads to more loops in topology detection, end bus reduction, critical bus reduction, as well as the conversion of the circuit back to a form which can be interpreted by a power flow solver. While the latter part is specific to the OpenDSS solver, it is expected to scale similarly for c[illegible]

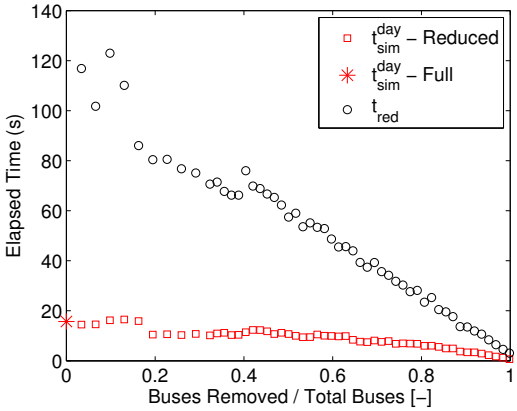

Fig. 8: Computation time to reduce the 621 bus feeder to a subset of CB (black) and the QSTS time (red) associated with the reduced feeder for simulating one day at 30 s timesteps. A different simulation set was used to control for time delays due to communication with external storage devices. The data points represent the average run times associated with 6 simulations each for a random selection of locations of CB. CB numbers were varied from 1 to 440 in increments of 10 and 440 to 620 in increments of 20.

V. Conclusion

A comprehensive method to reduce large realistic distribution feeders is proposed. The algorithm is sophisticated enough to handle complex configurations such as

TABLE I: Computational expense associated with reduction of the original feeder (t_{red}) and simulation of the reduced feeder (t_{sim}) as presented in Fig. 8. The yearly simulation time is extrapolated from the one-day simulation time for 30s time steps. The last column of data represents the ratio of time it took to simulate the reduced feeder to the full feeder for the extrapolated 1 year simulations. Note: The number of buses simulated will generally be greater than the number of user selected buses

User selected buses	% red.	t_{red} (s)	$t_{\mathrm{sim}}^{\mathrm{day}}$ (s)	$t_{\mathrm{sim}}^{\mathrm{year}}$ (min)	$1-\frac{t_{\mathrm{sim}}^{\mathrm{year_i}}}{t_{\mathrm{sim}}^{\mathrm{year_1}}}$
621 (Full)	-	-	15.68	95.4	-
500	20%	86.0	10.5	65.0	31%
400	36%	66.2	10.3	63.6	33%
300	52%	53.6	9.5	58.4	39%
200	67%	37.4	7.5	46.0	52%
100	84%	13.7	5.6	34.2	64%
50	92%	10.9	3.4	20.7	78%
20	96%	6.8	1.9	9.4	90%
10	98%	4.6	1.2	7.6	92%
1	99.8%	3.1	0.6	3.7	96%

1) multiphase connections through out the entire network
2) mutual coupling between multiphase unbalanced lines
3) unbalanced loads and generation
4) spatial variation in load and generation

through manipulation of the full impedance matrix. The method is also unique through the retention of geographic variance in both PV generation and load consumption by a phase and impedance-weighted impact.

A sensitivity analysis was performed on a real California distribution feeder, which accounted for differences in solar generation, load consumption, penetration level, load type, and number of CB. The algorithm is shown to maintain the CB voltages with a maximum error of 1.13% and an rMSE of 0.21% in bus voltage. The largest contributor to error was found to be the distance of the bus from the substation due to aggregation errors. The error is weakly correlated with the load type used in the simulation.

The reduction provides significant time savings. For example, greater than 90% reduction in simulation time was found for feeders which reduced the number of buses by at least 96%, while reducing only 20% of the total buses resulted in a 31% time savings for simulating one year at 30s time steps.

The potential critical buses for a distribution feeder include, but are not limited to, the buses which 1) host sensitive loads such as hospitals, 2) host voltage regulation devices such as smart inverters or capacitors, 3) host power flow controllers such as battery management systems, or 4) show maximum and minimum voltage magnitudes.

Future improvements to the method will focus on reducing the time associated with reduction, automation of CB selection, and handling of advanced distribution modeling elements. Consideration of distribution line shunt capacitance, reduction of secondary transformers, imperfect neutral grounding, and alternative forms of generation are essential to real world application. Further, even though it has been shown here to have little effect, a reduction scheme which does not rely on the constant current assumption will be developed.

References

[1] NYS Department OF Public Service and Staff Report AND Proposal, “Proceeding on Motion of the Commission in Regard to Reforming the Energy Vision DPS Staff Report and Proposal,” 2014.

[2] J. Smith, M. Rylander, L. Rogers, and R. Dugan, "It's all in the plans: Maximizing the benefits and minimizing the impacts of ders in an integrated grid," *IEEE Power Energy Mag.*, vol. 13, no. 2, pp. 20–29, 2015.

[3] M. Lave, M. J. Reno, and R. J. Broderick, "Characterizing local high-frequency solar variability and its impact to distribution studies," *Solar Energy*, vol. 118, pp. 327–337, 2015.

[4] A. Nguyen, M. Velay, J. Schoene, V. Zheglov, B. Kurtz, K. Murray, B. Torre, and J. Kleissl, "High PV penetration impacts on five local distribution networks using high resolution solar resource assessment with sky imager and quasi-steady state distribution system simulations," *Solar Energy*, vol. 132, pp. 221–235, jul 2016.

[5] V. R. Disfani, P. Ubiratan, and J. Kleissl, "Model predictive on-load tap changer control for high penetrations of pv using high resolution resources assessment with sky imager," in *2016 IEEE Power & Energy Society General Meeting*. IEEE, 2016, pp. 1–5.

[6] J. E. Quiroz, M. J. Reno, and R. J. Broderick, "Time series simulation of voltage regulation device control modes," in *Photovoltaic Specialists Conference (PVSC), 2013 IEEE 39th*. IEEE, 2013, pp. 1700–1705.

[7] Department of Energy, "Funding Opportunity Announcement: Enabling Extreme Real-Time Grid Integration of Solar Energy (ENERGISE)," 2016.

[8] G. Kron, *Tensor analysis of networks*. J. Wiley & Sons, 1939.

[9] W. W. Price, A. W. Hargrave, B. J. Hurysz, J. H. Chow, and P. M. Hirsch, "Large-scale system testing of a power system dynamic equivalencing program," *IEEE Trans. Power Syst.*, vol. 13, no. 3, pp. 768–774, 1998.

[10] H. Oh, "A new network reduction methodology for power system planning studies," *IEEE Trans. Power Syst.*, vol. 25, no. 2, pp. 677–684, 2010.

[11] B. V. Ramana, K. Murthy, P. U. Kumar, V. R. Kumar *et al.*, "A two bus equivalent method for determination of steady state voltage stability limit of a power system," *Int. J. Computat. Eng. Res*, vol. 2, pp. 428–434, 2012.

[12] D. Santos-Martin and S. Lemon, "Simplified Modeling of Low Voltage Distribution Networks for PV Voltage Impact Studies," *IEEE Trans. Smart Grid*, pp. 1–8, 2015.

[13] V. Valdivia, F. Gonzalez-Espin, D. Diaz, and R. Foley, "Low-frequency reduced-order modeling approach and implementation of grid emulation in hardware-in-the-loop platforms," in *Power Electronics and Applications (EPE'15 ECCE-Europe), 2015 17th European Conference on*. IEEE, 2015, pp. 1–7.

[14] A. Nagarajan and R. Ayyanar, "Application of minimum spanning tree algorithm for network reduction of distribution systems," in *North American Power Symposium (NAPS), 2014*. IEEE, 2014, pp. 1–5.

[15] J. Brochu, C. Larose, and R. Gagnon, "Generic equivalent collector system parameters for large wind power plants," *IEEE Trans. Energy Convers.*, vol. 26, no. 2, pp. 542–549, 2011.

[16] Y. Cheng, M. Sahni, J. Conto, S.-H. Huang, and J. Schmall, "Voltage-profile-based approach for developing collection system aggregated models for wind generation resources for grid voltage ride-through studies," *IET renewable power gen*, vol. 5, pp. 332–346, 2011.

[17] F. Ghassemi and K.-L. Koo, "Equivalent network for wind farm harmonic assessments," *IEEE Trans. Power Del.*, vol. 25, no. 3, pp. 1808–1815, 2010.

[18] J. V. Milanović and S. M. Zali, "Validation of equivalent dynamic model of active distribution network cell," *IEEE Trans. Power Syst.*, vol. 28, pp. 2101–2110, 2013.

[19] M. J. Reno, K. Coogan, R. Broderick, and S. Grijalva, "Reduction of distribution feeders for simplified pv impact studies," in *Photovoltaic Specialists Conference (PVSC), 2013 IEEE 39th*. IEEE, 2013, pp. 2337–2342.

[20] J. B. Ward, "Equivalent circuits for power-flow studies," *Electrical Engineering*, vol. 68, no. 9, pp. 794–794, 1949.

[21] R. Van Amerongen and H. Van Meeteren, "A generalised ward equivalent for security analysis," *IEEE Transactions on Power apparatus and Systems*, no. 6, pp. 1519–1526, 1982.

[22] A. Shapovalov, C. Spieker, and C. Rehtanz, "Network reduction algorithm for smart grid applications," in *Power Engineering Conference (AUPEC), 2013 Australasian Universities*. IEEE, 2013, pp. 1–5.

[23] Electric Power Research Institute (EPRI), "Distribution Green Circuits Collaboration," Tech. Rep., 2010.

[24] S. Deckmann, A. Pizzolante, A. Monticelli, B. Stott, and O. Alsac, "Numerical testing of power system load flow equivalents," *IEEE transactions on power apparatus and systems*, no. 6, pp. 2292–2300, 1980.

[25] S. M. Ashraf, B. Rathore, and S. Chakrabarti, "Performance analysis of static network reduction methods commonly used in power systems," in *Power Systems Conference (NPSC), 2014 Eighteenth National*. IEEE, 2014, pp. 1–6.

[26] S. Deckmann, A. Pizzolante, A. Monticelli, B. Stott, and O. Alsac, "Studies on power system load flow equivalencing," *IEEE transactions on power apparatus and systems*, no. 6, pp. 2301–2310, 1980.

[27] M. J. Reno, R. J. Broderick, and S. Grijalva, "Formulating a simplified equivalent representation of distribution circuits for pv impact studies," *Sandia National Laboratories SAND2013-2831*, 2013.

[28] V. R. Disfani, M. C. Bozchalui, and R. Sharma, "Sdp-based state estimation of multi-phase active distribution networks using micro-pmus," *arXiv preprint arXiv:1504.03547*, 2015.

[29] Z. Pecenak. (2017) Zack pecenak personal page. [Online]. Available: http://solar.ucsd.edu/c/people/zack-pecenak/

[30] R. C. Dugan and T. E. McDermott, "An open source platform for collaborating on smart grid research," in *Power and Energy Society General Meeting, 2011 IEEE*. IEEE, 2011, pp. 1–7.